

Bacterioplankton dynamics driven by interannual and spatial variation in diatom and dinoflagellate spring bloom communities in the Baltic Sea

María Teresa Camarena-Gómez ^{1,2*} Clara Ruiz-González ³ Jonna Piiparinen,¹ Tobias Lipsewiers,¹ Cristina Sobrino,⁴ Ramiro Logares,³ Kristian Spilling ^{1,5}

¹Marine Research Centre, Finnish Environment Institute, Helsinki, Finland

²Tvärminne Zoological Station, University of Helsinki, Hanko, Finland

³Institut de Ciències del Mar (ICM-CSIC), Barcelona, Spain

⁴Faculty of Science, University of Vigo, Vigo, Spain

⁵Department of Natural Sciences, University of Agder, Kristiansand, Norway

Abstract

In parts of the Baltic Sea, the phytoplankton spring bloom communities, commonly dominated by diatoms, are shifting toward the co-occurrence of diatoms and dinoflagellates. Although phytoplankton are known to shape the composition and function of associated bacterioplankton communities, the potential bacterial responses to such a decrease of diatoms are unknown. Here we explored the changes in bacterial communities and heterotrophic production during the spring bloom in four consecutive spring blooms across several sub-basins of the Baltic Sea and related them to changes in environmental variables and in phytoplankton community structure. The taxonomic structure of bacterioplankton assemblages was partially explained by salinity and temperature but also linked to the phytoplankton community. Higher carbon biomass of the diatoms *Achnanthes taeniata*, *Skeletonema marinoi*, *Thalassiosira levanderi*, and *Chaetoceros* spp. was associated with more diverse bacterial communities dominated by copiotrophic bacteria (Flavobacteriia, Gammaproteobacteria, and Betaproteobacteria) and higher bacterial production. During dinoflagellate dominance, bacterial production was low and bacterial communities were dominated by Alphaproteobacteria, mainly SAR11. Our results suggest that increases in dinoflagellate abundance during the spring bloom will largely affect the structuring and functioning of the associated bacterial communities. This could decrease pelagic remineralization of organic matter and possibly affect the bacterial grazers communities.

During the last decades, shifting phytoplankton spring bloom communities from diatom-dominated blooms toward higher abundances of dinoflagellates have been reported in some sub-basins of the Baltic Sea (Klais et al. 2011). This tendency seems to be due to certain climate change-related effects, such as increases in water temperature and in wind speed and decreases in the thickness of the ice-cover, which appear to favor the excystment of the cold-water dinoflagellates resting cysts that may dominate until the early summer (BACC II Author Team 2015; Legrand et al. 2015). Diatoms and dinoflagellates have different ecological traits, in terms of

growth rate (Spilling and Markager 2008), quality and quantity of dissolved organic matter (DOM) release (Mykkestad 1995), and sedimentation patterns (Heiskanen 1998). Heterotrophic bacteria are the main consumers of the DOM produced by phytoplankton in the Baltic Sea (Legrand et al. 2015; Lindh et al. 2015), and both diatoms and dinoflagellates have been associated to different bacterial communities (Pinhassi et al. 2004; Camarena-Gómez et al. 2018). Thus, understanding how the predicted changes in the nature of the Baltic Sea spring bloom may impact bacterial community composition and activity is essential to estimate any potential biogeochemical consequences of this global warming driven process.

The nature and the timing of the spring bloom in the Baltic Sea vary between the different sub-basins (Kahru and Nõmmann 1990). The bloom typically starts with light promoting net primary production (PP) in the southernmost Baltic Sea in February/March, reaching the Gulf of Finland (GoF) in April, and the Gulf of Bothnia in May. The bloom reaches the peak phase when inorganic nutrients have been depleted; N-limitation prevails in most of the Baltic Sea except for the P-limited Bay of Bothnia (Andersson et al. 1996; Tamminen and Andersen 2007). The

*Correspondence: m.t.camarena@gmail.com; teresa.camarena.gomez@environment.fi

This is an open access article under the terms of the Creative Commons Attribution License, which permits use, distribution and reproduction in any medium, provided the original work is properly cited.

Additional Supporting Information may be found in the online version of this article.

[Copyright line changed on 5 June 2021 after issue publication.]

subsequent decline phase is characterized by the rapid sinking of the phytoplankton cells (Heiskanen 1998). Therefore, understanding the bacterial responses to changes in phytoplankton communities requires considering the large environmental and spatiotemporal heterogeneity between sub-basins, that is, the timing of the bloom and the pronounced salinity (2–20) and temperature (0–20°C) gradients (Hagström et al. 2001).

Several studies in the Baltic Sea have shown that the taxonomic composition of bacterial communities varies along the salinity gradient with Alphaproteobacteria and Gammaproteobacteria dominating in more saline waters, whereas Actinobacteria, Betaproteobacteria, and Planctomycetes are favored by lower salinity (Rieck et al. 2015; Bunse et al. 2016). The strong seasonality in the Baltic Sea also shapes bacterial community structure and dynamics: Alphaproteobacteria are present throughout the year (Lindh et al. 2015; Rieck et al. 2015), Bacteroidetes (mainly class Flavobacteriia), and some taxa from Beta- and Gammaproteobacteria classes are associated with phytoplankton spring blooms (Hugerth et al. 2015; Bunse et al. 2016), Verrucomicrobia, Actinobacteria, and Planctomycetes appear in summer/autumn (Lindh et al. 2015). Although both the physico-chemical environment and biotic interactions affect bacterial communities, most of these studies have been restricted to specific sub-basins or did not capture the full development of the spring bloom, thus preventing a comprehensive understanding of bacterial responses at the whole Baltic Sea scale. A recent experimental study in the Baltic Sea showed that diatom-dominated treatments promoted the growth of copiotrophic bacterial groups such as Flavobacteriia or Gammaproteobacteria as well as increases in bacterial heterotrophic production compared to dinoflagellate-dominated treatments (Camarena-Gómez et al. 2018). However, so far, no study has addressed this issue in natural conditions or across the naturally occurring environmental gradients in the Baltic Sea.

The aim of this study was to investigate how differences in the taxonomic composition of phytoplankton spring bloom communities (diatom- or dinoflagellate-dominated) affect the community structure and dynamics of the associated bacterioplankton across different areas of the Baltic Sea. For that, we collected samples in four consecutive years (2013–2016) during different phases of the spring bloom (Growth, Peak, Decline, and Postbloom), from the northern Gulf of Bothnia to the southern Baltic Proper (BP). We explored changes in bacterioplankton communities and their heterotrophic production in relation to environmental variables (abiotic and phytoplankton communities). Based on our previous experimental studies (Camarena-Gómez et al. 2018), we hypothesized that dinoflagellate dominated communities will lead to less productive bacterial communities with reduced number of copiotrophic bacteria compared with diatom-dominated communities.

Material and methods

Study area, sampling design, and environmental variables

The water samples were collected during four cruises (April–May; 2013–2016) onboard R/V *Aranda*. In total, 127 stations

were sampled, and the area spanned from the southern BP (55°22'N) to the northern Bay of Bothnia (BoB, 65°53'N), also covering GoF, Åland Sea (ÅS), Archipelago Sea (ArS), and Bothnian Sea (BS) sub-basins (Table 1; Fig. 1A). Four samples were collected in the Kvarken region (bordering BoB and BS) and these were added to the BoB stations. The number of samples differed by sub-basin (Table 1). At all stations, the water was collected from 3 m depth either using an oceanographic rosette with Niskin bottles of 5 L ($n = 122$) or from the flow-through system on board ($n = 5$) in 2013.

Salinity, temperature, and depth were recorded in situ. Inorganic nutrients ($\text{NO}_2 + \text{NO}_3\text{-N}$, $\text{NH}_4\text{-N}$, $\text{PO}_4\text{-P}$, and dissolved silicate (DSi)) were analyzed by standard colorimetric methods (Grasshoff et al. 1983). Samples for chlorophyll *a* (Chl *a*) determination (100–200 mL) were filtered onto glass fiber filters (GF/F, pore size: 0.7 μm , Whatman) in duplicates. Chl *a* was extracted in 10 mL of ethanol (96% v/v) (Jespersen and Christoffersen 1987) and stored at –20°C until further determination with a fluorescence spectrophotometer (Agilent Cary Eclipse). Dissolved organic carbon (DOC) and dissolved organic nitrogen (DON) were analyzed from 0.2 μm filtered samples using a Shimadzu TOC-V CPH analyzer and following the temperature catalytic oxidation method (Benner et al. 1993).

Plankton community composition, biomass, and productivity

For the determination of nano- and microplankton, including phytoplankton, water samples (200 mL) were fixed with acid Lugol's solution on board and stored in darkness at 4°C until enumeration. Depending on the Chl *a* concentration, subsamples of 10–50 mL were used to enumerate the plankton species abundance and to measure cells biovolume with an inverted light microscope (Leitz DM IRB, Leica). The abundance was converted to carbon biomass as described by Lipsewiers and Spilling (2018). PP, defined as gross production during 2 h incubations, was determined by measuring the incorporation of ^{14}C -labeled sodium bicarbonate with a scintillation counter (Wallac 1414, Perkin Elmer) according to Steemann-Nielsen (1952). Total dissolved inorganic carbon (DIC) was determined using a high-temperature combustion IR carbon analyzer. The PP was calculated from the incorporated ^{14}C after incubation knowing the total amount of added isotope and the DIC concentration according to Gargas (1975). A more detailed description of the method can be found in Spilling et al. (2019).

The DOC released by phytoplankton cells was measured by filtering the total community onto 0.2 μm pore size polycarbonate filters after 24 h incubation with $\text{NaH}^{14}\text{CO}_3$ in a climate control room at surface water temperature (2–6°C). The percent extracellular release of ^{14}C (PER) was calculated based on the dissolved organic fraction ($\text{DO}^{14}\text{C} < 0.2 \mu\text{m}$) of the total ^{14}C fixation after incubation. Since substantial heterotrophic consumption of DOC (on average, 30–50%) might take

Table 1. Environmental (abiotic) variables measured along the four sampling transects (2013–2016): Temperature (Tem), salinity, nitrite + nitrate ($\text{NO}_2\text{-NO}_3$), ammonium (NH_4), phosphate (PO_4), dissolved silica (DSi), dissolved organic carbon (DOC), and nitrogen (DON). The table represents the range between the minimum and maximum values, indicated in bold, recorded for each variable and measured in each sub-basin. The different sub-basins covered are indicated: Gulf of Finland (GoF), Baltic Proper (BP), Åland Sea (ÅS), Archipelago Sea (ArS), Bothnian Sea (BS), and Bay of Bothnia (BoB) including Kvark stations. The different phytoplankton bloom phases are indicated: Growth (Gr), Peak (Pe), Decline (De) and Postbloom (PB), defined in more detail in Table S1. $N = 127$.

	# of stations	Sub-basin	Bloom phase	Tem (°C)	Salinity	$\text{NO}_2\text{-NO}_3$ ($\mu\text{mol L}^{-1}$)	NH_4 ($\mu\text{mol L}^{-1}$)	PO_4 ($\mu\text{mol L}^{-1}$)	DSi ($\mu\text{mol L}^{-1}$)	DOC (mmol L^{-1})	DON ($\mu\text{mol L}^{-1}$)
10–26 Apr 2013	31	GoF	Gr, Pe, De	0.76–1.98	5.09–6.38	0–5.85	0.10–0.39	0.19–0.48	7.84–19.75	0.30–1.08	10.06–45.57
05–10 May 2014	11	BP	Gr, Pe	1.62–2.72	5.97–7.24	0–2.08	0.04–0.19	0.06–0.33	8.27–14.24	0.41–1.01	13.49–30.78
	4	ÅS	Gr, Pe	1.29–1.59	5.45–6.16	0–2.59	0.07–0.13	0.02–0.35	8.92–13.10	0.35–0.51	16.07–17.85
	9	GoF	De, PB	4.25–5.18	5.03–6.01	0–0.26	0.5–0.24	0.12–0.33	2.27–9.10	0.50–1.05	16.07–28.70
	2	BP	De, PB	4.62–5.69	6.56–6.63	0	0.05	0.28	7.60–11.60	0.44–0.52	15.16–16.06
	4	ArS	De, PB	4.58–5.17	5.90–6.29	0–0.4	0.08–0.11	0.20–0.33	6.01–8.10	0.60–1.12	16.02–67.86
04–15 May 2015	5	GoF	De, PB	3.91–5.35	4.96–5.86	0–0.02	0.08–0.44	0.18–0.36	5.50–11.20	0.46–1.07	16.36–25.40
	6	ArS	Pe, PB	4.41–6.09	5.75–6.38	0–0.23	0.06–0.13	0.06–0.33	5.60–11.10	0.32–0.64	11.33–18.58
	4	ÅS	De	5.03–6.22	5.41–6.06	0	0–0.06	0.05–0.22	6.70–8.70	0.37–0.47	12.73–13.97
	4	BP	De, PB	4.52–5.69	5.72–6.56	0–0.44	0.05–0.34	0.27–0.40	7.6–11.8	0.37–0.55	15.16–18.95
	10	BS	Pe	3.59–4.16	5.12–5.54	0–0.38	0.05–0.13	0–0.21	8.10–12.70	0.33–1.07	12.40–18.66
04–15 Apr 2016	9	BoB	Pe, De	1.35–4.73	2.20–5.09	0–7.47	0.04–0.35	0–0.02	9.40–55.70	0.35–0.68	15.73–55.53
	4	GoF	Gr, Pe, De	1.56–2.89	4.95–5.20	0–6.64	0.14–0.22	0.34–0.61	12.21–19.09	0.44–0.58	14.71–31.52
	20	BP	Gr, Pe, De, PB	2.47–5.90	5.92–7.77	0–1.89	0–1.19	0.16–0.57	11.77–17.65	0.32–0.62	10.73–22.10
	4	ÅS	Pe	2.84–3.28	5.51–5.68	0–0.17	0.11–0.18	0.12–0.18	15.57–18.17	0.34–0.99	12.40–14.54

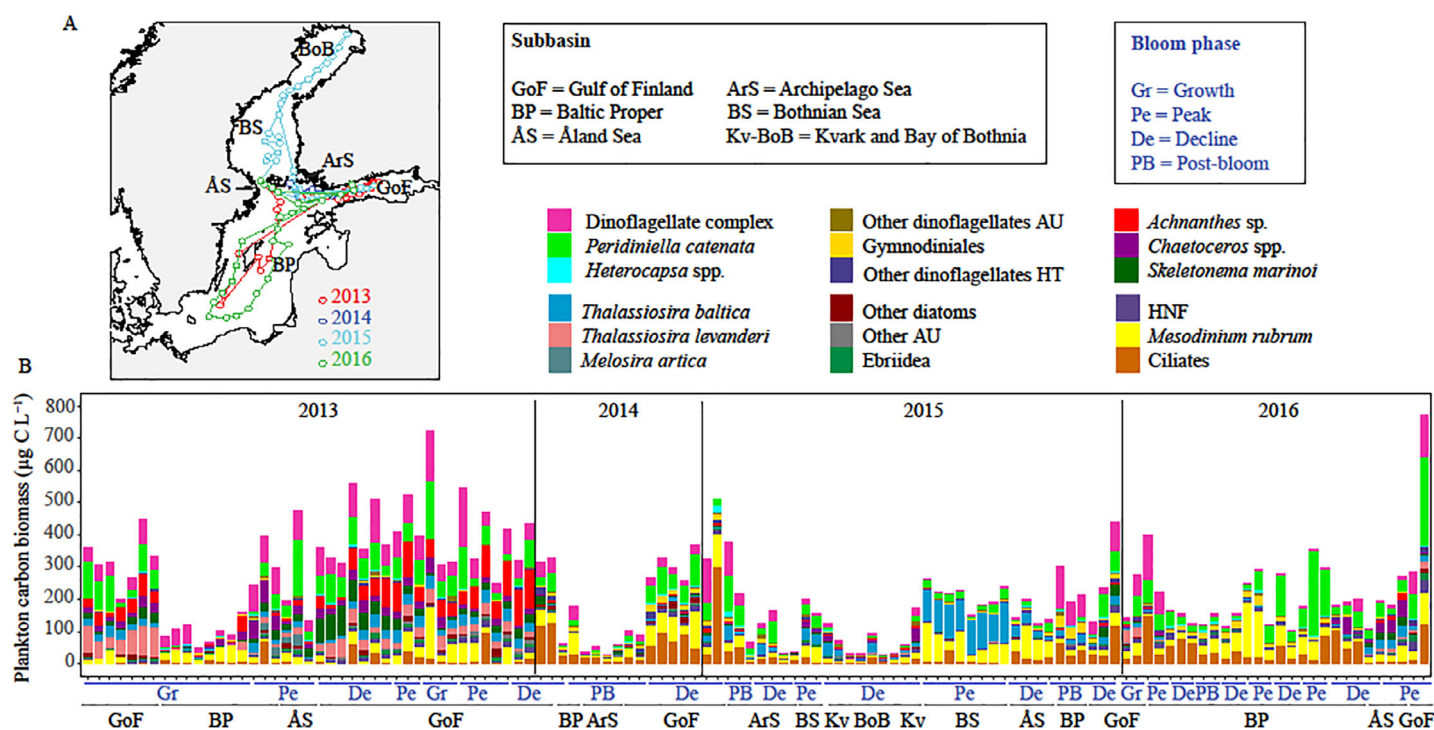


Fig 1. (A) Sampling transects during the 4 yr: 2013 (red), 2014 (dark blue), 2015 (light blue), and 2016 (green). The sub-basins covered are indicated in the map and the abbreviations are explained in the black box. (B) Plankton dynamics measured as carbon biomass during the 4 yr. The X-axis shows the bloom phases (blue) and the sub-basins (black) through the sampled stations ($N = 122$). The lines separate the different sampling years. The legend remarks groups that contributed more to the total biomass. AU, autotrophs; HT, heterotrophs.

place during the incubation period (Morán and Estrada 2002), the results are regarded as net DOC production rates.

Different phases of the spring bloom, named as Growth (Gr), Peak (Pe), Decline (De), and Postbloom (PB) were defined for each station and sampling year, as described in detail in Spilling et al. (2019). In brief, the phases were defined based on the concentration of inorganic nutrients (PO_4 and $\text{NO}_3 + \text{NO}_2$) and Chl *a* (Supporting Information Table S1). The $\text{NO}_3 + \text{NO}_2$ was used for the N-limited sub-basins GoF, BP, ArS, ÅS, and BS; and PO_4^{3-} for the P-limited BoB sub-basin. High Chl *a* was defined as within 20% of the average peak concentration during spring, which is different in the different sub-basins (Supporting Information Table S1).

Bacterial heterotrophic production

Bacterial production estimated as thymidine (BPT) and leucine (BPL) uptake were measured in triplicates (1 mL sample) by using the dual labeling with [methyl- ^3H]-thymidine and [^{14}C (U)]-leucine at final saturating concentrations of 20 nmol L^{-1} and 166 nmol L^{-1} , respectively. One sample was fixed with formaldehyde (final concentration 1.85%) and was used as a blank. The samples were incubated at in situ temperature during 2 h in darkness. The incubation was stopped by the addition of formaldehyde. The samples were processed using the cold trichloroacetic acid extraction method (Fuhrman and Azam 1982) and the centrifugation method

(Smith and Azam 1992). The thymidine incorporation was converted to carbon production ($\mu\text{g C L}^{-1} \text{ h}^{-1}$), using a cell conversion factor of 1.4×10^9 cells nmol^{-1} (HELCOM 2008) and a carbon conversion factor using the formula of $0.12 \text{ pg C} \times (\mu\text{m}^3 \text{ cell}^{-1})^{0.7}$ (Norland 1993). We assumed a bacterial cell volume of $0.06 \mu\text{m}^3$, which corresponds to the mean cell volume of bacteria previously measured during spring blooms in the Baltic Sea (Kuparinen and Kuosa 1993). The leucine incorporation was converted to carbon production using a factor of $1.5 \text{ kg C mol}^{-1}$ (Simon and Azam 1989).

Bacterial abundance

Bacterial abundances (BA) were determined in duplicates (1.2 mL sample) by flow cytometry according to Gasol and del Giorgio (2000). The samples were fixed with paraformaldehyde (final concentration 1%) and incubated 10 min in darkness and stored at -80°C until further analysis. The counts were done by staining the cells with SYBER Green I (Sigma-Aldrich) and counting them with a Partec-CUBE flow cytometer as described in Camarena-Gómez et al. (2018).

Bacterial community composition

Samples for bacterial community analysis (500 mL) were gravity-filtered onto sterile $0.2 \mu\text{m}$ pore-size Whatman cellulose ester filters, which were stored at -80°C until further analysis. DNA was extracted using the Power Soil DNA

isolation kit (Mo Bio Laboratories). We amplified the 16S ribosomal RNA (rRNA) gene, V1–V3 hypervariable region. We used a two-step polymerase chain reaction with the universal primers F27 (AGAGTTTGATC[ACTG]TGGCTCAG) and R519 (GTATTACCGCGGCTGCTG) (Lane 1991). Amplicons were subsequently paired-end sequenced on an Illumina MiSeq platform, using multiplexing at the Institute of Biotechnology, University of Helsinki, Finland. The processing of the sequences was done according to the pipeline described by Logares (2017). In brief, primers were removed with Cutadapt (Martin 2011). The paired-end reads were merged with PEAR (Zhang et al. 2014). Quality filtering (> 400 bp, maximum expected errors = 1), chimera checking, and operational taxonomic unit (OTU) clustering (99% similarity) were done with the UPARSE pipeline (Edgar 2013). In total, 4.22 million sequences passed the quality filtering. After the removal of singletons as well as chloroplasts and mitochondria, based on the classification with SILVA v123, 2247 OTUs and 2.25 million reads were retained. Samples with less than 7000 reads (four samples) were removed. The remaining samples (122) were normalized by rarefaction using *rrarefy* in R (R Development Core Team 2008) to the lowest number of reads ($n = 7024$ reads). Downstream analyses were carried out using the rarefied data, including 122 samples and 2128 OTUs.

The DNA sequencing data has been submitted to ENA (European Nucleotide Archive) under the accession number PRJEB37659.

Statistical analyses

Bacterial community turnover was analyzed comparing the similarity between samples. A Bray-Curtis dissimilarity matrix was generated and used for nonmetric multidimensional scaling (NMDS) analyses using the *metaMDS* function of the R package *vegan*. Taxonomic richness was estimated with the Chao 1 index and taxonomic diversity with Shannon index. Significant differences in bacterial heterotrophic production, bacterial abundance, and Shannon index between the different sampling years and phytoplankton bloom phases were assessed applying nonparametric tests: Kruskal–Wallis for comparing the samples and Wilcoxon rank-sum test as a post hoc test.

Heterogeneity in the measured local environmental variables (biotic and abiotic) was compared against community turnover (Bray-Curtis dissimilarity) by means of Mantel linear correlations (*mantel.test* function, R package *ade*). The distance matrices of the environmental variables, *z*-score transformed, were constructed by computing the Euclidean distances of either all abiotic variables (salinity, temperature, dissolved oxygen, inorganic nutrients, dissolved inorganic and organic carbon), or single abiotic variables (salinity and temperature), or by computing the Bray-Curtis distances of the biotic variables: whole phytoplankton assemblages, or only the diatom communities, or only the dinoflagellate communities.

The effect of the environmental variables (explanatory variables) on the structure of the studied bacterioplankton communities was further assessed by applying a redundancy analysis (RDA, maximum 200 permutations) with forward selection (R package *vegan*) to obtain the abiotic or biotic variables that significantly explain the bacterial community variance (response variable). The variables selected for the RDA analysis were all the environmental variables included in the Mantel tests. Prior to the analysis, the variables were normalized by calculating the *z*-scores. The RDA forward selection analysis included an ANOVA test in each step (permutation test for RDA under reduced model, permutations: free, number of permutations: 999) to identify the significant environmental variables ($p < 0.05$). Collinearity between the explanatory variables was tested before and after the analysis to exclude the highly correlated variables by using the variance inflation factors (VIFs); only variables with $VIF < 10$ were retained for further analysis. The significant explanatory variables were used to construct the final model and the results were presented in an RDA plot. A variation partitioning analysis was performed to explore which portion of the variation in bacterial community structure could be explained by either the biotic (plankton communities) or the abiotic variables. This was done considering all the data together ($N = 122$ samples) or each year individually (2013–2016) and constructing two explanatory matrices representing the abiotic component and the planktonic (biotic) component, which included the variables that had been previously selected with the forward selection analysis. Spearman correlations were used to compare the relative abundances of specific bacterial groups with bacterial production, bacterial abundance, and variations in environmental variables (abiotic or biotic) using the R package *ggpubr*. The results of the correlation analysis were presented in a Heatmap by using the R package *ComplexHeatmap*. All figures and analyses were performed in R (R Development Core Team 2008).

Results

Environmental variation and plankton bloom dynamics

The environmental conditions varied largely within and between the sampling years due to the different sub-basins and phytoplankton bloom phases covered (Table 1; Fig. 1A, Spilling et al. 2019). Salinity ranged from ~ 8 in the southernmost station of the BP to ~ 2 in the northernmost part of the BoB sub-basin (Table 1). Temperature was generally low ($< 2^\circ\text{C}$) in 2013, which had high inorganic nutrient concentrations and all the sub-basins in this year were mainly in Growth and Peak bloom phases (Table 1). The stations where the temperature was $> 4^\circ\text{C}$ had low inorganic nutrient concentrations and were in Decline and Postbloom phase (e.g., in 2014 and 2015). Exceptionally, BoB sub-basin had high nitrite + nitrate ($\text{NO}_2^- + \text{NO}_3^-$) concentrations ($4\text{--}7.5 \mu\text{mol L}^{-1}$), similar to the concentrations found during

Table 2. Biological variables measured along the four sampling transects (2013–2016): Chl *a*, PP, percentage of extracellular release (PER), bacterial heterotrophic production, measured as leucine (BPL) and thymidine (BPT) incorporations rates, bacterial abundance, and Shannon index of the bacterial community. The table shows the range between the minimum and maximum values (indicated in bold), recorded for each variable and measured in each sub-basin. The sub-basin abbreviations are defined in Table 1.

	Sub-basin	Chl <i>a</i> ($\mu\text{g L}^{-1}$)	PP ($\mu\text{g L}^{-1} \text{ h}^{-1}$)	PER	BPT ($\mu\text{g L}^{-1} \text{ h}^{-1}$)	BPL ($\mu\text{g L}^{-1} \text{ h}^{-1}$)	BA (10^6 cell mL^{-1})	Shannon index
10–26 Apr 2013	GoF	10.26–21.96	13.01– 61.18	0.58–3.62	0.26–0.51	0.16– 0.62	0.20 –0.67	2.91 – 4.61
	BP	2.22–11.54	3.16–17.64	1.92–6.62	0.18–0.52	0.07–0.33	0.23–0.69	3.73–4.38
	ÅS	6.10–12.73	12.28–21.32	1.39–2.08	0.43–0.57	0.17–0.43	0.46–0.59	3.82–4.23
05–10 May 2014	GoF	2.40–10.33	4.58–28.72	4.38–19.28	0.44– 1.67	0.11–0.43	1.11–1.94	4.21–4.45
	BP	1.52–1.91	4.47–6.44	2.27–25.84	0.73–1.14	0.20–0.33	0.89–1.64	3.89–4.31
	ArS	0.70 –2.29	3.21–5.78	6.61–7.99	1.03–1.59	0.19–0.33	1.67–2.03	4.29–4.41
04–15 May 2015	GoF	3.19–12.56	5.44–17.70	0.28 –5.78	0.29–0.47	0.15–0.31	2.57–4.09	3.51–3.68
	ArS	1.66–8.90	3.39–14.79	2.19–6.41	0.17–0.25	0.08–0.11	2.64–4.54	3.40–3.56
	ÅS	2.88–4.82	4.04–5.50	1.58–2.66	0.10–0.21	0.06–0.25	2.62–2.93	3.42–3.48
	BP	2.88–6.57	3.39–13.21	2.16–8.57	0.17–0.28	0.09–0.13	1.73–3.22	3.21–3.58
	BS	6.35–12.91	4.19–22.65	0.94–4.15	0.08 –0.18	0.04 –0.13	1.58–3.46	3.59–3.82
	BoB	1.62–6.79	1.01 –4.54	2.67–9.95	0.10–0.70	0.04–0.44	1.27– 4.87	3.15–3.88
04–15 Apr 2016	GoF	9.36– 26.07	5.64–22.41	3.07–13.97	0.14–0.28	0.09–0.32	1.95–2.86	3.39–3.53
	BP	1.66–11.97	2.09–11.02	5.91– 21.97	0.08–0.25	0.05–0.17	0.72–2.48	2.42–3.34
	ÅS	7.42–10.16	10.42–20.37	7.89–15.31	0.16–0.19	0.10–0.12	2.41–3.15	3.24–3.41

the Growth phase of the bloom, and the phosphate (PO_4) was almost depleted after the bloom. The lowest DSi concentration ($2.27 \mu\text{mol L}^{-1}$) was measured in the GoF in 2014, while the maximum DSi concentration ($\sim 55 \mu\text{mol L}^{-1}$) was detected in the Kemi river plume in the northernmost BoB (Table 1). The DOC and DON showed the highest concentrations in the ArS in 2014 (DOC: $> 1 \text{ mmol L}^{-1}$; DON: $68 \mu\text{mol L}^{-1}$), and the lowest in the GoF in 2013 (DOC: 0.30 mmol L^{-1} ; DON: $10.06 \mu\text{mol L}^{-1}$). High Chl *a* concentrations ($> 20 \mu\text{g L}^{-1}$) were observed in the GoF sub-basin during the Growth and Peak bloom phases (Table 2) and coinciding with the stations that presented high phytoplankton carbon biomass (Fig. 1B). The highest PP was also measured in the GoF and largely in 2013 ($61 \mu\text{g L}^{-1} \text{ h}^{-1}$, Table 2). The percentage extracellular release (PER) was opposite to the PP, increased in the Decline and Postbloom phases and was higher in the BP compared to the other sub-basins (Table 2).

Overall, the planktonic communities, including mostly phytoplankton and nano-microzooplankton, were largely dominated by diatoms, dinoflagellates, the mixotrophic *Mesodinium rubrum*, and heterotrophic ciliates, contributing $> 80\%$ to the total carbon biomass (Fig. 1B, Supporting Information Fig. S1). Diatom biomass decreased from the Growth bloom phase (38% total carbon) to the Postbloom phase ($< 5\%$ total carbon), whereas dinoflagellate biomass was similar in all bloom phases ($\sim 33\%$ total carbon) and heterotrophic organisms increased toward the postbloom phase (Supporting Information Fig. S1A). When comparing the different sampling years, a much higher total biomass

($> 300 \mu\text{g C L}^{-1}$) was observed in 2013 than in the other 3 yr. In addition, the biomass in 70% of the communities in 2013 was largely dominated by diatoms ($> 140 \mu\text{g C L}^{-1}$) and dinoflagellates ($110 \mu\text{g C L}^{-1}$; Fig. 1B), coinciding with the early spring bloom (mainly Growth and Peak phases). In the other years, dinoflagellates had higher biomass than diatoms (Fig. 1B). For instance, the dinoflagellate biomass in 2014 and 2016 were $> 90 \mu\text{g C L}^{-1}$ in 40% of the stations, which also displayed more heterotrophic organisms such as ciliates and the heterotrophic dinoflagellate group Gymnodiniales, named also as Dinoflagellates HT, coinciding with a later bloom phase (Fig. 1B; Supporting Information Fig. S1A). Heterotrophic nanoflagellates (HNF) contributed most to the total biomass in 2016 ($> 10 \mu\text{g C L}^{-1}$; Fig. 1B) and mainly during the late bloom phase (Supporting Information Fig. S1). The silicoflagellate *Ebria tripartita* (fam. Ebriidae) represented a small fraction of the biomass but contributed more to the total biomass in 2013 than in the other years (Fig. 1B) and mainly in the sub-basins with a high abundance of diatoms (GoF and ArS; Supporting Information Fig. S1B). The contribution of other autotrophic plankton organisms, such as Cryptophyceae, Chrysophyceae, Euglenophyceae, Prasinophyceae, Chlorophyceae, and Nostocophyceae, to the total biomass was generally low ($< 1\%$; Supporting Information Fig. S1).

Within diatoms, *Achnanthes taeniata*, *Skeletonema marinoi*, *Thalassiosira levanderi*, and *Chaetoceros* spp. were the dominant species (Fig. 1B). In the BS sub-basin, only the Peak phase was sampled (Table 1) and the single diatom *Thalassiosira baltica* dominated the community (Fig. 1B). Autotrophic dinoflagellates were dominated by the dinoflagellate complex (a group

of species difficult to identify by the traditional microscopy method), most likely formed by *Biecheleria baltica* and/or *Gymnodinium corollarium*, in the GoF and BP sub-basins (Fig. 1B, Supporting Information Fig. S1B). The chain-forming *Peridiniella catenata* was present across the four sampling years. Other autotrophic dinoflagellates (e.g., *Heterocapsa* spp.) and heterotrophic/mixotrophic dinoflagellates (e.g., *Protoperidinium* spp. and *Dinophysis* spp., respectively) were also detected, but their contribution to the total plankton biomass was low (< 5%).

Bacterioplankton community structure and its environmental drivers

The taxonomic composition of the studied bacterial communities varied largely across the stations sampled (Fig. 2A). Overall, Alphaproteobacteria, mainly SAR11, dominated in all the sampling years, being present in all the sub-basins and bloom phases (Fig. 2A; Supporting Information Fig. S2). The classes belonging to the Phylum Bacteroidetes (Flavobacteriia, Sphingobacteriia and Cytophagia) had higher relative abundance during 2013 and 2014 than in the other years. The class Flavobacteriia dominated within Bacteroidetes and comprised on average ~25% of the total sequences (Fig. 2A). Within Flavobacteriia, the genus *Flavobacterium* contributed 8–12% to the total reads in 2013. Other Flavobacteriia genera such as *Fluviicola*, *Polaribacter*, and *Owenweeksia* also contributed to

the community. Gammaproteobacteria dominated by the genus *Crenothrix* contributed 10–15% of the communities sampled in 2013 (Fig. 2A) and, in general, in the GoF and AS sub-basins (Supporting Information Fig. S2B) but decreased, even more acutely than Flavobacteriia, as the bloom progressed (Supporting Information Fig. S2A). Betaproteobacteria, largely dominated by the BAL58 marine group, showed higher relative abundance (5–7%) in 2013 and 2014 than in 2015 and 2016 (Fig. 2A). The classes Actinobacteria (hgcl clade) and Acidimicrobiia (CL500-29 marine group) had higher relative abundance in 2014 compared to the other years, reaching values of 12.73% and 9%, respectively (Fig. 2A). Actinobacteria were found mainly to be associated with the late bloom phases (Supporting Information Fig. S2A). The phylum Phycisphaerae (CL500-3) showed generally low abundances in all the bloom phases but reached its highest values (11.03%) in the BoB (Fig. 2A; Supporting Information Fig. S2B), sampled only in 2015.

Based on their overall taxonomic structure, the bacterial communities clustered into two groups differing largely in taxonomic richness (Chao 1; Fig. 2B) and diversity (Shannon index; Table 2). The group with significantly higher taxonomic diversity comprised all communities sampled during 2013 and 2014 (Wilcoxon; $p < 0.0001$; Table 2), which were characterized by higher relative abundances of Flavobacteriia, Sphingobacteriia, Cytophagia, Beta- and Gammaproteobacteria, and Actinobacteria. The low taxonomic richness group, sampled in 2015–2016, was clearly

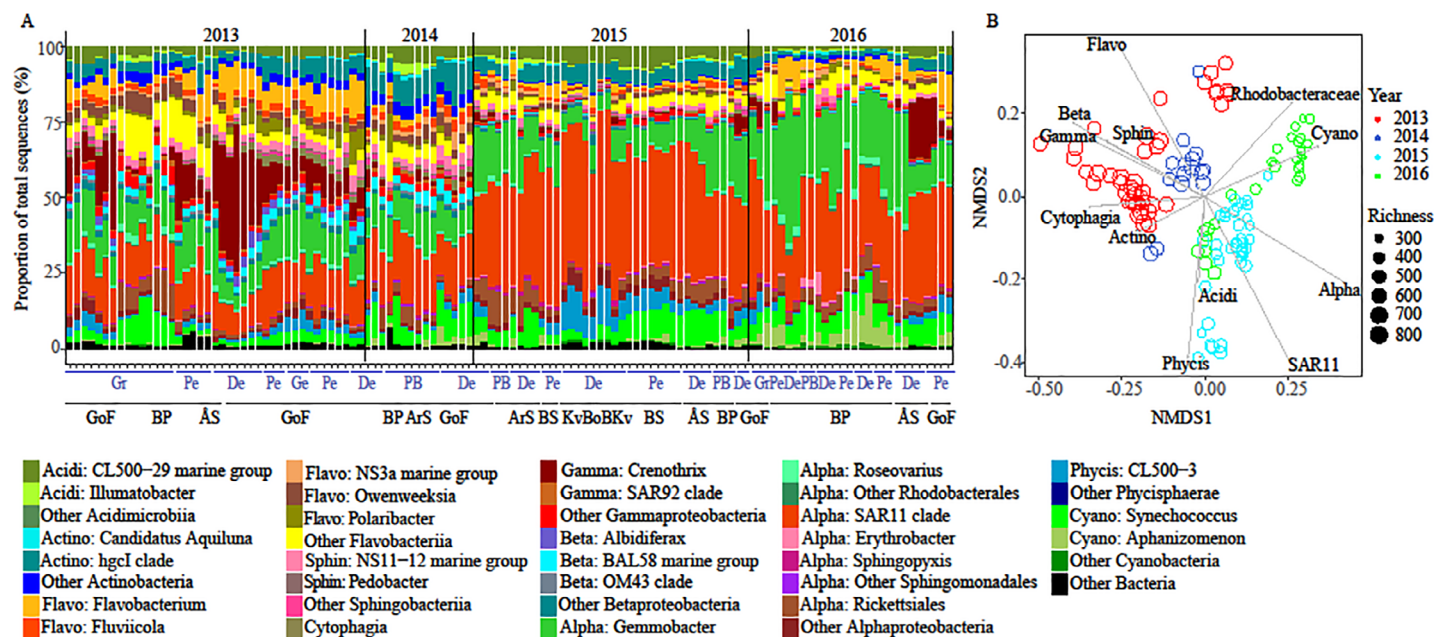


Fig 2. Bacterial community composition (A) across the 4 yr (2013–2016). The X-axis shows the bloom phases (blue) and the sub-basins (black) through the sampled stations (N = 122) and the abbreviations are defined in Table 1 and in Fig. 1. The Y-axis indicated the relative abundance of the bacterial taxa. Only the bacterial groups that contributed more than 0.25% of the total sequences are indicated in the legend and the rest are grouped as “other bacteria.” The classification was performed at the class or genus level in most cases, but the class Alphaproteobacteria was split into the main orders Rhodobacterales and SAR11. The lines separate the different sampling years. (B) NMDS of bacterial community structure based on Bray-Curtis dissimilarity (N = 122, stress = 0.134). The color indicates the sampling year and the dot size is proportional to the OTU richness (Chao 1) in each community. The vectors indicate the main bacterial groups found in the 4 yr, corresponding to those shown in panel (A).

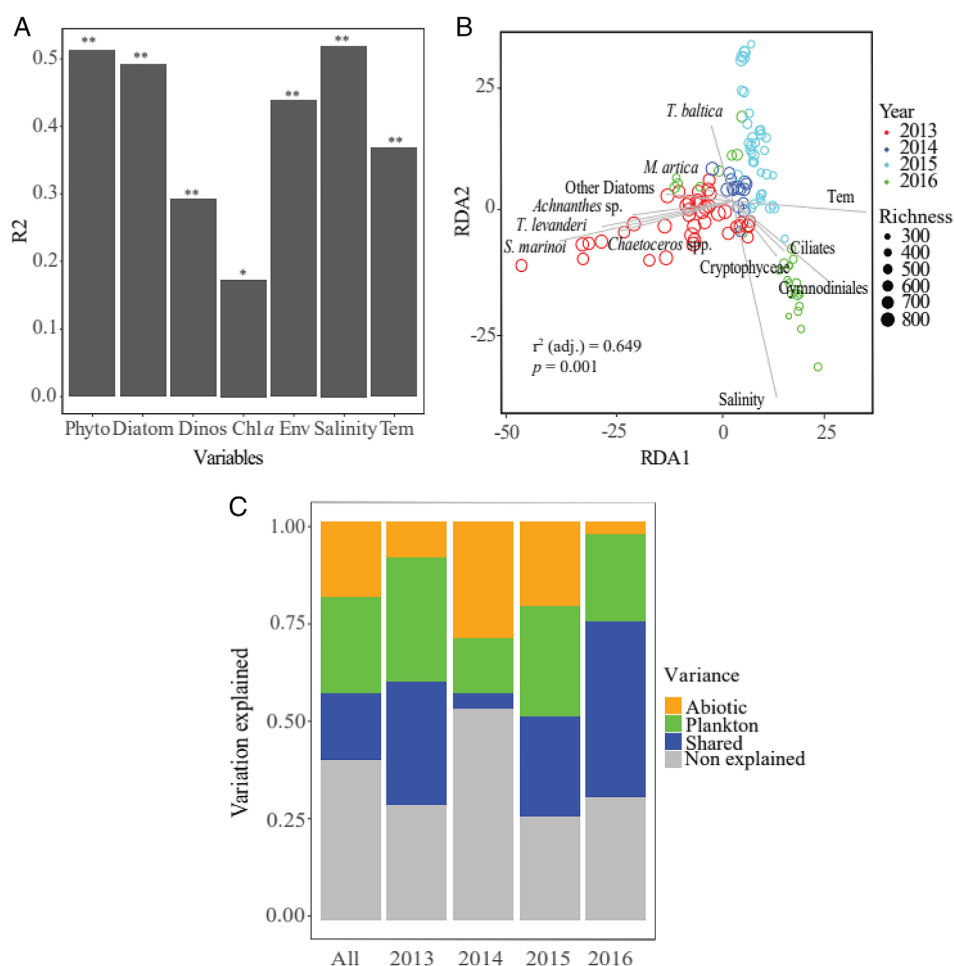


Fig 3. Link between bacterial community structure and environmental variables across the four sampled years. **(A)** R coefficients of the mantel correlations between differences in environmental (abiotic or plankton) variables and bacterial Bray-Curtis community structure dissimilarity matrices, pooling all samples together ($N = 122$). The dissimilarity matrices compared include taxonomic dissimilarities of the total phytoplankton communities (Phyto), of the diatom communities (diatom), and the dinoflagellate communities (Dinos), Chl *a*, all physical-chemical variables (salinity, temperature, dissolved oxygen, inorganic nutrients, dissolved inorganic and organic carbon), salinity, and temperature (tem). ** $p < 0.001$, * $p < 0.01$. **(B)** RDA of the bacterial community including the explanatory significant environmental variables selected with the RDA forward selection: Salinity and temperature (tem), the biomass of *A. taeniata*, *S. marinoi*, *T. levanderi*, *Chaetoceros* spp., *T. baltica*, *Melosira artica*, other diatoms, Cryptophyceae, Gymnodiniales and ciliates. The R^2 value (R_{adj}) and the p value (ANOVA-like permutation test) represent the most parsimonious model. the color indicates the sampling years (as in Fig. 1) and the dot size is proportional to the OTU richness (Chao 1) in each community. **(C)** Results of partial regression analysis including the variables selected from the RDA forward selection, partitioning the variation in bacterial community composition considering all the samples together (all) and each sampling year. Four different components are shown: Abiotic variation (orange) independent of plankton community; variation due to changes in planktonic communities (green) independent of any abiotic factors; variation attributable to a combination of plankton and abiotic factors (blue); unexplained variation (gray).

dominated by Alphaproteobacteria (SAR11 and Rhodobacteriaceae) and Cyanobacteria (Fig. 2B). The taxonomic diversity was also significantly higher during the Growth bloom phase (Wilcoxon; $p < 0.001$) compared with the other bloom phases, whereas no significant differences were found between the other bloom phases (Wilcoxon; $p > 0.05$; Supporting Information Fig. S3A). Differences in bacterial community composition were significantly correlated with differences in environmental variables, mainly with salinity (Mantel $R = 0.52$, $p < 0.001$; Fig. 3A) and temperature

gradients (Mantel $R = 0.37$; $p < 0.001$), as well as with differences in the phytoplankton community composition (Mantel $R = 0.51$; $p < 0.001$). The high correlation found between differences in phytoplankton and bacterial community composition seemed to be mostly due to changes in diatom communities, as suggested by the higher Mantel R found when comparing with diatoms (Mantel $R = 0.492$, $p < 0.001$), than with dinoflagellates (Mantel $R = 0.292$, $p < 0.001$; Fig. 3A). Interesting, the correlation between changes in the bacterial assemblages and those in Chl *a* concentration was lower

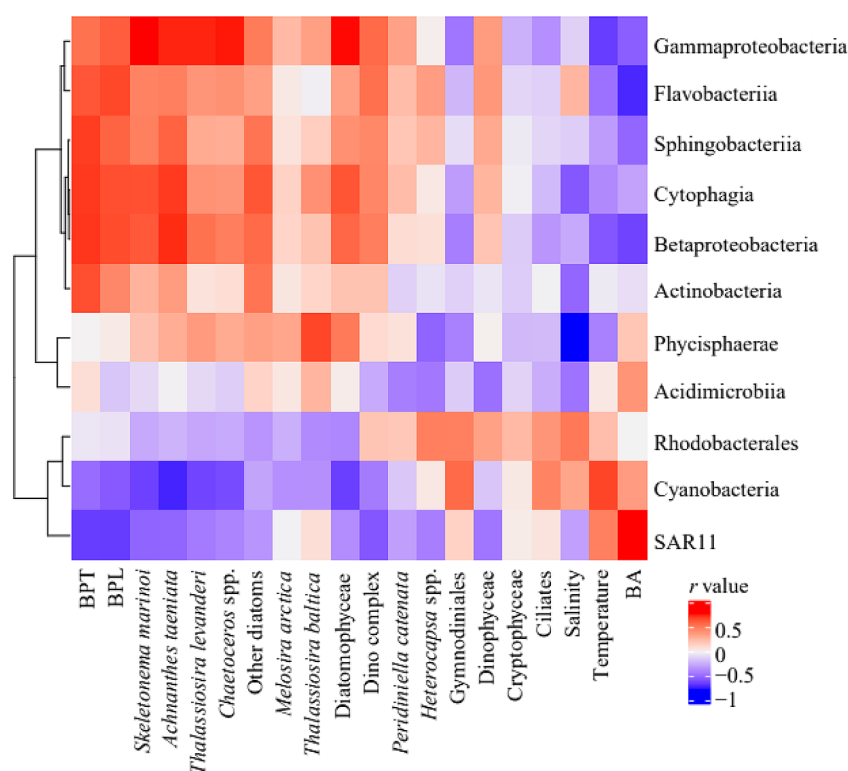


Fig 4. Heatmap of correlations between the relative abundance of the main bacterial groups and: Bacterial heterotrophic production measured as leucine uptake (BPL) and thymidine uptake (BPT); bacterial abundance (BA); the biomass of diatom and dinoflagellate groups, including all diatoms (Diatomophyceae) and autotroph dinoflagellates (Dinophyceae); and the rest of the significant environmental variables selected from the forward selection from the RDA analysis. The color indicates the spearman correlation coefficients (rho values). $N = 122$.

(Mantel $R = 0.17$, $p < 0.01$) than the correlation found between bacterial and phytoplankton dissimilarity matrices. A more detailed analysis on the effect of the environmental variables on the bacterial community composition revealed that, together with the abiotic variables (temperature and salinity), the abundances of several phytoplankton groups significantly explained the observed variation in bacterial communities (Fig. 3B). For example, lower temperatures and the presence of several diatom species such as *A. taeniata*, *S. marinoi*, *T. levanderi*, and *Chaetoceros* spp. shaped the bacterial communities in 2013, whereas the salinity gradient seemed to differentiate communities from 2015 and 2016, together with the biomass of the diatom *T. baltica*. Higher abundances of organisms, such as Cryptophyceae and some heterotrophs organisms like Gymnodiniales, ciliates and HNF, were associated with the bacterial communities sampled during 2016 (Fig. 3B).

These results were supported by the variation partitioning analysis demonstrating that both, the abiotic (salinity and temperature) and biotic variables (plankton community) influenced the variance in taxonomic composition when pooling all the data together, explaining 19% and 24% of the variance, respectively (Fig. 3C). However, when the different sampling years were considered separately, we observed a stronger effect of the plankton community than the abiotic

variables on the bacterial community structure in all the sampling years except in 2014 (Fig. 3C).

Environmental drivers of major bacterioplankton groups

We then explored the individual relationships between different abiotic and biological factors and the abundances of the main bacterial groups. The relative abundances of Flavobacteriia, Cytophagia, Sphingobacteriia, Gamma- and Betaproteobacteria were positively correlated with bacterial heterotrophic production, with all the diatoms species, except *M. arctica*, and also with the dinoflagellate complex (Fig. 4). Conversely, they were negatively correlated with the carbon biomass of Cryptophyceae, heterotrophic organisms (Gymnodiniales and ciliates), temperature, and salinity (Fig. 4). Only Flavobacteriia correlated positively with salinity. SAR11 and Cyanobacteria correlated positively with temperature and with bacterial abundance in the case of SAR11, whereas the dominance of certain diatoms or autotrophic dinoflagellates caused decreases in their relative abundances (Fig. 4). SAR11 also correlated negatively with salinity, whereas Rhodobacterales showed positive correlations. Phycisphaerae correlated positively with the biomass of the diatom *T. baltica*.

When exploring the relationship between the bacterial groups and all diatoms or dinoflagellates together, Gammaproteobacteria was the group showing the strongest positive correlation ($R = 0.751$, $p = 0.0001$) with the total

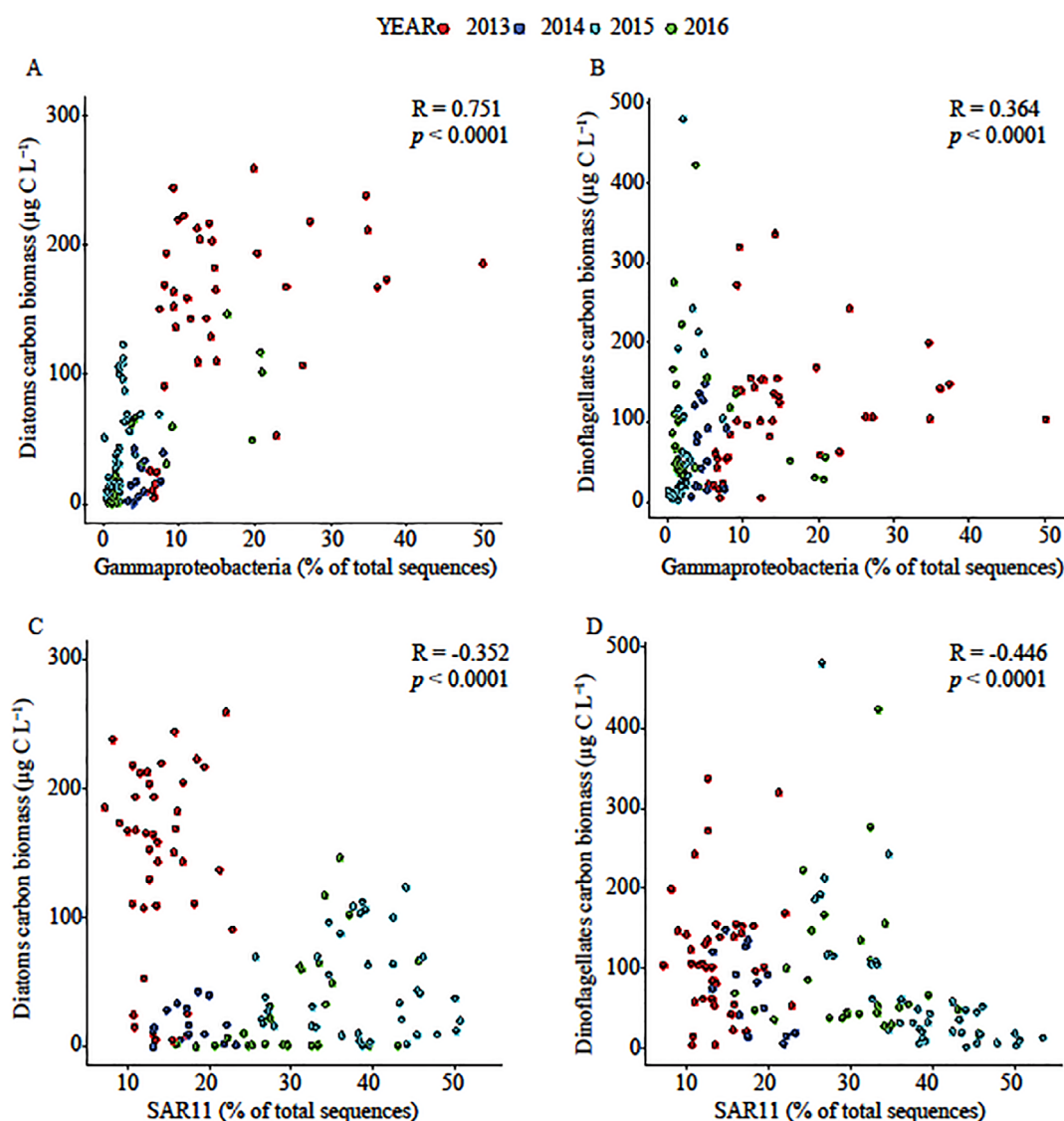


Fig 5. Spearman correlations between diatom or dinoflagellate biomass and the relative abundance (%) of Gammaproteobacteria (**A**, **B**) and SAR11 (**C**, **D**) pooling all the samples together ($N = 122$). The color of the dots indicates the sampling years. Rho correlation coefficients and significance level (p values) are presented in the figures.

biomass of diatoms (Fig. 5A), being also positive with dinoflagellates (Fig. 5B). In contrast, SAR11 was the group showing the strongest negative correlation with the total biomass of diatoms ($R = -0.364$, $p = 0.0001$; Fig. 5C) and dinoflagellates ($R = -0.456$, $p = 0.0001$; Fig. 5D). Betaproteobacteria, Cytophagia, and Sphingobacteria also correlated positively and greatly with diatoms compared to dinoflagellates (Supporting Information Table S2), and more specifically with the diatom groups *S. marinoi*, *A. taeniata*, *Chaetoceros* spp., and *T. levanderi* (Supporting Information Table S3).

Links between bacterial community structure and prokaryotic heterotrophic activity

Overall, the bacterial production rates measured with leucine incorporation (BPL) were significantly higher in 2013 and

2014 compared with 2015 and 2016 (Wilcoxon: $p < 0.0001$), similarly to the Shannon diversity values (Table 2). The greatest value of BPL was measured in 2013 ($0.62 \mu\text{g C L}^{-1} \text{ h}^{-1}$; Table 2), following the tendency of the PP (Table 2). When bacterial heterotrophic production was measured as thymidine incorporation (BPT), the rates were significantly higher in 2014 (Wilcoxon: $p < 0.0001$) than in the other years, reaching values of $1.67 \mu\text{g C L}^{-1} \text{ h}^{-1}$ (Table 2). No significant differences were found in BPL (Kruskal–Wallis; chi-squared = 1.1544, $\text{df} = 3$, $p = 0.764$) and BPT (Kruskal–Wallis; chi-squared = 7.3596, $\text{df} = 3$, $p = 0.06128$) between bloom phases (Supporting Information Fig. S3B,C). In contrast, the highest bacterial abundances (BA) were recorded at the stations sampled in 2015 and the lowest in 2013 (Wilcoxon: $p < 0.0001$; Table 2). The bacterial abundance was also significantly lower

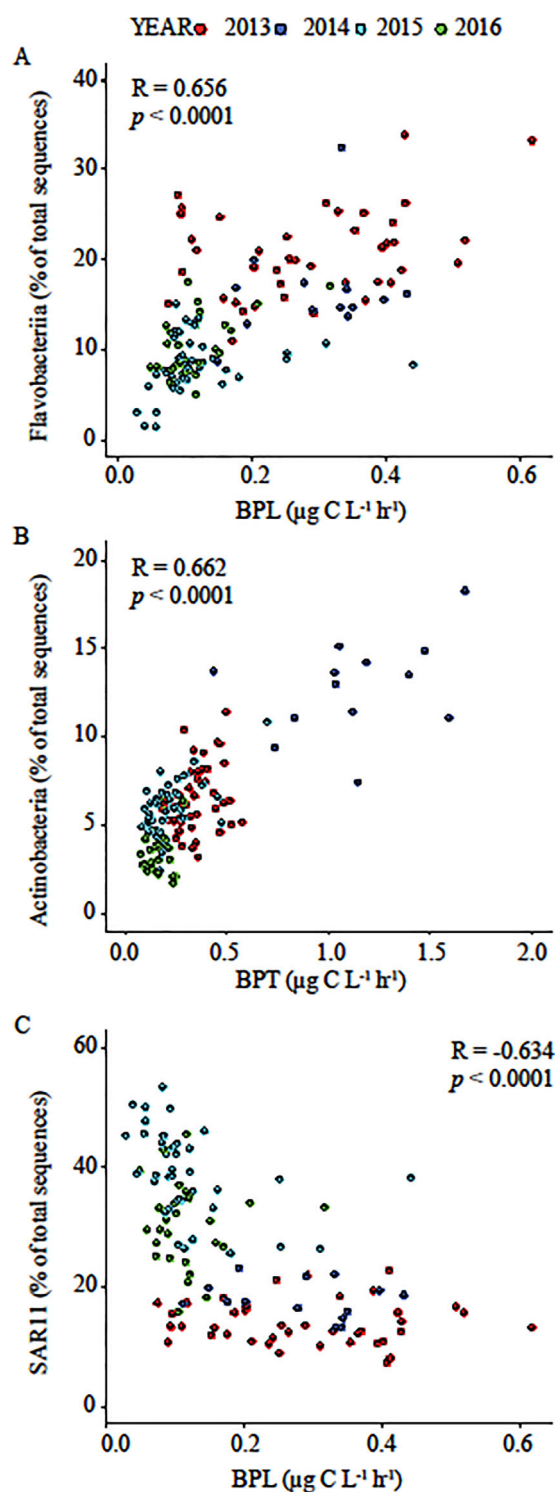


Fig 6. Spearman correlation between bacterial production measured as leucine uptake (BPL) or thymidine uptake (BPT) and the relative abundance (%) of Flavobacteriia (A), Actinobacteria (B), and SAR 11 (C) during the study ($N = 122$). The color of the dots indicates the sampling years. Rho correlation coefficients and significance level (p values) are presented in the figure.

during the Growth phase compared with the other bloom phases (Wilcoxon: $p < 0.001$; Supporting Information Fig. S3D), opposite to the pattern shown by the Shannon diversity index.

Interestingly, the differences in bacterial community composition found across our data set seemed to have an impact on community functioning. For example, most of the bacterial groups that were prevalent in the high diversity assemblages in 2013 and 2014, that is, Flavobacteriia, and Actinobacteria, showed strong positive correlations with BPL ($R = 0.656$, $p = 0.0001$; Fig. 6A) and BPT ($R = 0.662$, $p = 0.0001$; Fig. 6B), respectively, coinciding with the highest bacterial production rates (Table 2). Also, Cytophagia, Sphingobacteria, Beta- and Gammaproteobacteria showed positive correlations with bacterial production rates (Supporting Information Table S2), whereas the abundance of SAR11 correlated negatively (BPL: $R = -0.634$, $p = 0.0001$; Fig. 6C; Supporting Information Table S2).

Discussion

Our results demonstrate that the structure of the studied bacterioplankton communities from the Baltic Sea, besides being affected by the interannual and spatial variation in salinity and temperature, is also strongly influenced by the nature of phytoplankton communities, and in particular, by the abundance of specific diatom species. As we captured much higher biomass of diatoms in 2013 than in the other years, the spatiotemporal heterogeneity covered by the sampling allowed us to explore how changes in the dominant phytoplankton groups, mainly diatoms and dinoflagellates, may be translated into changes in the structure and functioning of the associated bacterioplankton communities.

Spatiotemporal variability in environmental variables and plankton communities

Our large-scale sampling allowed covering highly heterogeneous phytoplankton communities spanning most bloom phases, ranging from those with a codominance of diatoms and dinoflagellates, to those largely dominated by dinoflagellates. During the early bloom development, particularly in the GoF, the water was cold with high inorganic nutrient concentrations, and the phytoplankton community was dominated by diatoms that typically occur during the cold-water season (Lignell 1990; Spilling 2007). The dominance of diatoms was also associated with high primary productivity suggesting an actively growing community. The increased availability of inorganic nutrients and light after the ice cover disappears are known to boost and shape the bloom dynamics in terms of Chl *a* concentration, primary productivity, and dominant phytoplankton species in the Baltic Sea (Tamminen and Andersen 2007). In the Bothnian Sea, which we sampled during the Peak growth phase, the phytoplankton community was dominated by the diatom species *T. baltica* along with

high biomass of the mixotrophic ciliate *M. rubrum*, both of which seem to be common in this sub-basin (Andersson et al. 1996). The diatom-dominated communities co-occurred to a varying extent with several dinoflagellates, most likely *G. corollarium* and *B. baltica* (Sundström et al. 2009; Olli and Trunov 2010) in the GoF and the BP, similarly to earlier observations (Klais et al. 2011). The heterotrophic *E. tripartita* was most abundant during diatom dominance, likely because it grazed on diatom species such as *Skeletonema* sp. and *Thalassiosira* spp., as previously reported (Hargraves 2002).

During the declining phytoplankton bloom, mainly sampled in 2014 and 2016, the water was warmer, and dinoflagellates contributed more to the biomass than diatoms. This is the typical situation in the GoF with diatoms being more abundant in early spring and autotrophic dinoflagellates gradually becoming more dominant as the nutrients are depleted (Heiskanen 1998; Spilling et al. 2018). For instance, the stations sampled in 2014 had low phytoplankton biomass and low DSi concentration in the GoF, suggesting that a diatom-dominated bloom had settled out of the surface layer before the time of sampling. In the BoB, the low phytoplankton biomass was limited by phosphate with excess $\text{NO}_2 + \text{NO}_3$ and DSi. This sub-basin is P-limited (Tamminen and Andersen 2007) and is more turbid due to terrestrial DOM inputs limiting light penetration and thus, resulting in light-limited PP (Andersson et al. 2015).

The abundance of nano- and microzooplankton such as heterotrophic nanoflagellates, ciliates, and heterotrophic dinoflagellates increased toward the decline phase, pointing to a more heterotrophic community. A decrease in phytoplankton biomass and an increase in the proportion of dinoflagellates and heterotrophic organisms have been projected for a future, warmer Baltic Sea (Legrand et al. 2015), in addition to the earlier onset of the spring bloom (Andersson et al. 2015). Remarkably, our results reflect different temperature scenarios, as although roughly the same sub-basins were sampled in 2013 and 2016, the stations in 2016 were warmer and the bloom was clearly in a more advanced stage, in line with these predictions.

Environmental variables drive bacterioplankton dynamics in the Baltic Sea

As hypothesized, the changes in the phytoplankton community composition between the different bloom phases and sub-basins were accompanied by pronounced shifts in the structure of the associated bacterial communities. This is in line with previous experimental (Pinhassi et al. 2004; Sarmiento et al. 2013) and field studies (Teeling et al. 2012; Lindh et al. 2015) of phytoplankton blooms. The release of phytoplankton-derived DOM during these blooms can lead to changes in bacterial community dynamics (Buchan et al. 2014).

The studied bacterial communities clustered into two clearly different groups characterized by high and low taxonomic richness and diversity, which corresponded to the

communities sampled during 2013–2014, and those sampled during 2015–2016, respectively. Among the environmental variables tested, salinity and temperature were the only abiotic variables significantly explaining the observed structural shifts in bacterial assemblages, but only the temperature gradient seemed to explain the observed partition between high and low richness communities. Salinity and temperature are known to be relevant factors in shaping the bacterial communities in the Baltic Sea (Hugerth et al. 2015; Herlemann et al. 2016). Thus, the predicted increases in water temperature and decrease in salinity due to an increase in water run-off along the Baltic Sea may lead to significant changes in the planktonic assemblages (Andersson et al. 2015; Legrand et al. 2015).

Besides abiotic factors, the biomass of specific diatom species such as *A. taeniata*, *Chaetoceros* spp., *S. marinoi*, and *T. levanderi* emerged as some of the most important environmental drivers explaining the segregation of high- and low-richness bacterial communities. More precisely, changes in diatom communities were more strongly related to taxonomic dissimilarities in bacterial assemblages than temperature variations, as shown by the Mantel tests. The important role of the diatom community on explaining the variation in the bacterial community composition was backed-up also by the variation partitioning analysis, showing that diatoms explained 24% of the variation in bacterial assemblages. It is thus possible that the diatom bloom captured in 2013 and the diatom bloom that had likely recently settled out from the surface layer in 2014, favored a higher diversity of associated bacterial communities with high abundances of groups such as Gamma- and Betaproteobacteria, Flavobacteriia, Sphingobacteriia, and Cytophagia. This was further supported by the strong and positive correlations between the different diatom groups and the abundances of these copiotrophic bacteria. These bacteria are known to be associated with the diatom blooms (Amin et al. 2012; Camarena-Gómez et al. 2018; Liu et al. 2019), in accordance with their preference for productive or bloom-like conditions. In contrast, the lower diatom biomass observed during 2015 and 2016 was associated with less diverse communities dominated by the SAR11 in 2015 and also by Rhodobacterales in 2016. This was supported by the strong negative correlations between the relative abundances of these bacterial groups and the total biomass of phytoplankton. The conditions within the less productive stations sampled in 2015 and 2016 likely promoted the dominance of SAR11, which typically dominates nutrient-poor environments (Alonso-Sáez et al. 2007). Other groups like Phycisphaerae, and in particular CL500-3, were negatively affected by salinity, in accordance with a previous study where Phycisphaerae was associated to the lower salinity of the Gulf of Bothnia and to a higher influence of allochthonous DOM (Rieck et al. 2015).

Within copiotrophic bacteria, the contribution of Gammaproteobacteria and Flavobacteriia differed between sampling years and bloom phases. Flavobacteriia were always present with fluctuating relative abundance, whereas

Gammaproteobacteria, dominated by the genus *Crenothrix*, peaked locally and decreased toward the collapse of the phytoplankton bloom in stations with complex diatom communities. The presence of *Crenothrix* was surprising in the surface waters since this taxon has been observed in anoxic bottoms in the Baltic Sea (Koskinen et al. 2011) and also in stratified lakes (Oswald et al. 2017). In addition, Flavobacteriia and Gammaproteobacteria have been reported to occupy different niches in terms of their metabolic capacities: Flavobacteriia are capable of degrading high-molecular weight compounds, such as proteins, chitin, and polysaccharides (Teeling et al. 2012), whereas Gammaproteobacteria are more specialized on breaking down low-molecular weight substrates during increased organic and inorganic substrate availability (Gómez-Consarnau et al. 2012). This may explain the occurrence of *Crenothrix* in our samples since this taxon is a methane-oxidizer bacteria specialized in the uptake of simple carbon compounds such as methane or acetate (Stoecker et al. 2006). This taxon may have benefited from the increase of the suitable substrates, either by fresh and labile DOM released or as a product from a metabolic cascade after the degradation process carried out by other bacterial groups.

We observed lower net PER measured during the cruise in 2013, coinciding with a dominance of diatoms and higher bacterial production rates, compared with the higher net PER detected during the 2016 cruise dominated by dinoflagellates and with lower bacterial production rates. This may suggest that diatoms release more labile DOC relative to particulate organic carbon (POC) production than dinoflagellates and that this diatom released-DOM was rapidly consumed by bacteria. This type of response agrees with previous studies conducted in the Baltic Sea showing that some diatoms species release more DOC than flagellates (Wolter 1982; Lignell 1990). However, PER might vary largely and be affected to some extent by bacterial consumption, but also by the physiology of the phytoplankton cells and/or by the different phases of the bloom (Mykkestad 1995; Morán and Estrada 2002), making difficult to conclude whether lower PER means higher heterotrophic activity. Besides the stimulation of certain bacteria by the release of DOM, phytoplankton and prokaryotic organisms are capable of interacting in many ways and can establish species-specific relationships that can be beneficial or harmful (Amin et al. 2012). Indeed, we observed negative correlations between major bacterial groups and the abundance of specific phytoplankton groups. For instance, the production of certain aldehydes by *Thalassiosira* spp. (Wichard et al. 2005) negatively affect the protein production of Bacteroidetes (Balestra et al. 2011). This could explain the low relative abundance of Flavobacteriia observed in the presence of the diatom *T. baltica* in the BS. Antibacterial effects of phytoplankton are not well studied, but there are indications that some species inhibit bacterial growth (Amin et al. 2012).

Links between bacterial community composition and ecosystem functioning

The observed changes in bacterial community structure resulted in pronounced changes in the bacterial heterotrophic production of the studied assemblages. Most stations sampled in 2013 and 2014 showed much higher rates of bacterial production based on the incorporation of leucine (BPL) compared to the stations sampled in 2015 and 2016. The BPL rates were similar or, in some cases, higher than those reported by previous studies conducted at similar temperatures during the spring in the Baltic Sea (Lindh et al. 2015; Bunse et al. 2019). The variation in BPL between studies conducted at similar temperatures might be due to the different dominating phytoplankton groups that produce DOM of diverse lability, but also to differences in the frequency of sampling at the studied sub-basins. For instance, Bunse et al. (2019) found large BPL values during a spring dinoflagellate-dominated bloom in the BP, whereas the BPL values we observed during a dinoflagellate bloom in 2016 dominated by *P. catenata* in the same sub-basin were half of the values they reported. This emphasizes the importance of the phytoplankton community composition as a driver of the bacterial carbon cycling mediated by the presence of specific bacterial taxa.

The higher values of BPL in our study coincided with the high richness of the bacterial communities in 2013 and 2014 and with the high abundances of copiotrophic groups such as Betaproteobacteria, Gammaproteobacteria, and Flavobacteriia associated with diatom dominance. In addition, large peaks in bacterial production based on the incorporation of thymidine (BPT) were observed in 2014 indicating an actively dividing community. This was mostly related to the increases in the relative abundance of Actinobacteria, which is known to occur after phytoplankton blooms (Hugerth et al. 2015) and to correlate positively with thymidine incorporation (Pérez et al. 2010). Gammaproteobacteria and Bacteroidetes are quickly grazed by heterotrophic nanoflagellates due to their preference to graze on actively growing bacteria (Alonso-Sáez et al. 2007). This may explain the low bacterial abundance of the active community observed in 2013. In contrast, SAR11 correlated negatively with BPL and positively with bacterial abundance which agrees with the small cell size and slow-growing pattern of this clade, typically occurring in oligotrophic ecosystems, and which seem capable to avoid grazing (Alonso-Sáez et al. 2007). These bacterial responses agree with those observed in a mesocosm study performed with water sampled in the Baltic Sea, where the growth of diatoms promoted higher bacterial production and higher dominance of Flavobacteriia, Gammaproteobacteria, and Cytophagia than the presence of dinoflagellates (Camarena-Gómez et al. 2018).

It is interesting to note that the highest diversity of the bacterial assemblages was not only found during the period dominated by copiotrophic bacteria (Gammaproteobacteria, Betaproteobacteria, and Flavobacteriia), during early bloom

phases or in the presence of diatoms, but also during postbloom phases, dominated by Actinobacteria, and in both cases associated with higher bacterial production rates. This suggests the occurrence of a bacterioplankton succession that responds to the increase of diatom-derived DOM by the increase in the bacterial production rates, but also responds to a niche partitioning of the highly diverse bacterial community that exploits different resources. Other studies have also reported higher bacterial diversity during the spring bloom dominated by diatoms in the Baltic Sea and Southern Ocean (Lindh et al. 2015; Liu et al. 2019). However, there are also contradictory findings with, for example, lower diversity with an increase in Chl *a* during a *Phaeocystis antarctica* bloom (Richert et al. 2019) and also lower diversity with an increase in PP (Raes et al. 2011). These contrasting results when comparing species diversity and ecosystem functioning might be linked to the different environmental circumstances in each study. For instance, differences in physico-chemical conditions, different spatial-temporal scales, nature of the phytoplankton community, or bloom conditions and differences in the sampling effort may lead to specific diversity-functioning relationships that cannot be easily predicted.

The bacterial remineralization of elements is critical for marine ecosystem functioning. The primary producers benefit from recycled nutrients and bacterial fixed carbon can be channeled to higher trophic levels through the microbial loop. Structural changes to bacterial communities and metabolism could consequently have profound effects on the fate and cycling of carbon within planktonic food webs. Our results link microbial community structure and function in the Baltic Sea to ongoing shifts in the phytoplankton community structure (Lindh and Pinhassi 2018). The data suggest that specific diatoms release high-quality DOM that enhances the growth of copiotrophic bacteria with high production rates, in turn favoring the recycling of carbon through the microbial loop. In contrast, the predicted increase in dinoflagellate abundance associated with warmer winters and springs in the Baltic Sea, seems to shift the bacterial community towards more oligotrophic generalist and reduce the bacterial production rates. This could have direct consequences for the bacterial grazers communities, affecting the transfer of carbon to higher trophic levels, and for pelagic nutrient remineralization, processes that may in turn be directly affected by changes in other environmental variables.

Conclusions

We found pronounced differences in the bacterial community composition and functioning driven by gradients in salinity and temperature, but also by differences in phytoplankton community composition. The positive correlations found between specific diatom species and the highly diverse bacterial copiotrophic communities as well as high bacterial heterotrophic activity emphasize a major role of diatom-derived DOM for bacterial remineralization of organic carbon. As such, our

results supported our hypothesis of less productive bacterial communities dominated by other than copiotrophic bacterial groups during dinoflagellate dominance. However, the bacterioplankton response was linked more strongly to changes in phytoplankton at the species than at the group level, as the largest shifts in bacterial community structure were explained by the presence of specific diatom species such as *A. taeniata*, *S. marinoi*, *T. levanderi*, and *Chaetoceros* spp. Changes in the carbon biomass of these species explained the variability in bacterioplankton communities to a larger extent than the steep gradients in salinity and temperature. This suggests that quantitative data at a fine phytoplankton taxonomic resolution are needed to understand the role of phytoplankton communities in shaping bacterial ecology. Finally, our results emphasize that the projected shifts in spring bloom dynamics could cause changes in bacterial mediated carbon fluxes in the Baltic Sea.

References

- Alonso-Sáez, L., and others. 2007. Bacterial assemblage structure and carbon metabolism along a productivity gradient in the NE Atlantic Ocean. *Aquat. Microb. Ecol.* **46**: 43–53. doi:[10.3354/ame046043](https://doi.org/10.3354/ame046043)
- Amin, S. A., M. S. Parker, and E. V. Armbrust. 2012. Interactions between diatoms and bacteria. *Microbiol. Mol. Biol. Rev.* **76**: 667–684. doi:[10.1128/MMBR.00007-12](https://doi.org/10.1128/MMBR.00007-12)
- Andersson, A., S. Hajdu, P. Haecky, J. Kuparinen, and J. Wikner. 1996. Succession and growth limitation of phytoplankton in the Gulf of Bothnia (Baltic Sea). *Mar. Biol.* **126**: 791–801. doi:[10.1007/BF00351346](https://doi.org/10.1007/BF00351346)
- Andersson, A., and others. 2015. Projected future climate change and Baltic Sea ecosystem management. *Ambio* **44**: 345–356. doi:[10.1007/s13280-015-0654-8](https://doi.org/10.1007/s13280-015-0654-8)
- BACC II Author Team. 2015. Second assessment of climate change for the Baltic Sea Basin in regional climate studies. Springer. doi:[10.1007/978-3-319-16006-1](https://doi.org/10.1007/978-3-319-16006-1)
- Balestra, C., L. Alonso-Sáez, J. M. Gasol, and R. Casotti. 2011. Group-specific effects on coastal bacterioplankton of polyunsaturated aldehydes produced by diatoms. *Aquat. Microb. Ecol.* **63**: 123–131. doi:[10.3354/ame01486](https://doi.org/10.3354/ame01486)
- Benner, R., and others. 1993. Measurement of dissolved organic carbon and nitrogen in natural waters: Workshop report. *Mar. Chem.* **41**: 5–10. doi:[10.1016/0304-4203\(93\)90101-S](https://doi.org/10.1016/0304-4203(93)90101-S)
- Buchan, A., G. R. LeCleir, C. A. Gulvik, and J. M. González. 2014. Master recyclers: Features and functions of bacteria associated with phytoplankton blooms. *Nat. Rev. Microbiol.* **12**: 686–698. doi:[10.1038/nrmicro3326](https://doi.org/10.1038/nrmicro3326)
- Bunse, C., and others. 2016. Spatio-temporal interdependence of bacteria and phytoplankton during a Baltic Sea spring bloom. *Front. Microbiol.* **7**: 517. doi:[10.3389/fmicb.2016.00517](https://doi.org/10.3389/fmicb.2016.00517)
- Bunse, C., S. Israelsson, F. Baltar, M. Bertos-Fortis, E. Fridolfsson, C. Legrand, E. Lindehoff, M. V. Lindh, S.

- Martínez-García, and J. Pinhassi. 2019. High frequency multi-year variability in baltic sea microbial plankton stocks and activities. *Front. Microbiol.* **9**. doi:[10.3389/fmicb.2018.03296](https://doi.org/10.3389/fmicb.2018.03296)
- Camarena-Gómez, M. T., and others. 2018. Shifts in phytoplankton community structure modify bacterial production, abundance and community composition. *Aquat. Microb. Ecol.* **81**: 149–170. doi:[10.3354/ame01868](https://doi.org/10.3354/ame01868)
- Edgar, R. C. 2013. UPARSE: Highly accurate OTU sequences from microbial amplicon reads. *Nat. Methods* **10**: 996–998. doi:[10.1038/nmeth.2604](https://doi.org/10.1038/nmeth.2604)
- Fuhrman, J., and F. Azam. 1982. Thymidine incorporation as a measure of heterotrophic bacterioplankton production in marine surface waters: Evaluation and field results. *Mar. Biol.* **66**: 109–120. doi:[10.1007/BF00397184](https://doi.org/10.1007/BF00397184)
- Gargas, E. 1975. A manual for phytoplankton primary production studies in the Baltic. Baltic Marine Biologists Publication No. 2. Water Quality Institute.
- Gasol, J. M., and P. A. Del Giorgio. 2000. Using flow cytometry for counting natural planktonic bacteria and understanding the structure of planktonic bacterial communities. *Sci. Mar.* **64**: 197–224. doi:[10.3989/scimar.2000.64n2197](https://doi.org/10.3989/scimar.2000.64n2197)
- Gómez-Consarnau, L., M. V. Lindh, J. M. Gasol, and J. Pinhassi. 2012. Structuring of bacterioplankton communities by specific dissolved organic carbon compounds. *Environ. Microbiol.* **14**: 2361–2378. doi:[10.1111/j.1462-2920.2012.02804.x](https://doi.org/10.1111/j.1462-2920.2012.02804.x)
- Caspers H. 1985. K. Grasshoff, M. Ehrhardt, K. Kremling (Editors): *Methods of Seawater Analysis*. Second, Revised and Extended Edition.—With 108 figs, 26 tab., 419 pp. Weinheim/Deerfield Beach, Florida: Verlag Chemie 1983. ISBN 3–527-2599-8 (Weinheim) 0–89573-7 (Deerfield Beach). DM 140,00, \$ 70.00. *Internationale Revue der gesamten Hydrobiologie und Hydrographie* **70**: (2) 302–303. doi:[10.1002/iroh.19850700232](https://doi.org/10.1002/iroh.19850700232)
- Hagström, Å., F. Azam, J. Kuparinen, and U. L. Zweifel. 2001. Pelagic plankton growth and resource limitations in the Baltic Sea, p. 177–210. *In* F. V. Wulff, L. A. Rahm, and P. Larsson [eds.], *A systems analysis of the Baltic Sea. Ecological studies (analysis and synthesis)*, v. **148**. Springer. doi:[10.1007/978-3-662-04453-7_7](https://doi.org/10.1007/978-3-662-04453-7_7)
- Hargraves, P. E. 2002. The ebridian flagellates *Ebria* and *Hermesinum*. *Plankton Biol. Ecol.* **49**: 9–16.
- Heiskanen, A. 1998. Factors governing sedimentation and pelagic nutrient cycles in the northern Baltic Sea. *Monogr. Boreal Env. Res.* **8**. Finnish Environment Institute. <http://hdl.handle.net/10138/39314>
- Helsinki Commission (HELCOM). 2008. Programme for monitoring of eutrophication and its effects. Annex C-11 guidelines concerning bacterioplankton growth determination. *In* *Manual for marine monitoring in the COMBINE programme of HELCOM*. Annex C-1:9. HELCOM.
- Herlemann, D. P. R., D. Lundin, A. F. Andersson, M. Labrenz, and K. Jürgens. 2016. Phylogenetic signals of salinity and season in bacterial community composition across the salinity gradient of the baltic sea. *Front. Microbiol.* **7**. doi:[10.3389/fmicb.2016.01883](https://doi.org/10.3389/fmicb.2016.01883)
- Hugerth, L. W., J. Larsson, J. Alneberg, M. V. Lindh, C. Legrand, J. Pinhassi, and A. F. Andersson. 2015. Metagenome-assembled genomes uncover a global brackish microbiome. *Genome Biol.* **16**: (1) doi:[10.1186/s13059-015-0834-7](https://doi.org/10.1186/s13059-015-0834-7)
- Jespersen, A. M., and K. Christoffersen. 1987. Measurements of chlorophyll a from phytoplankton using ethanol as extraction solvent. *Arch. Hydrobiol.* **109**: 445–454.
- Kahru, M., and S. Nömmann. 1990. The phytoplankton spring bloom in the Baltic Sea in 1985, 1986: Multitude of spatio-temporal scales. *Cont. Shelf Res.* **10**: 329–354. doi:[10.1016/0278-4343\(90\)90055-Q](https://doi.org/10.1016/0278-4343(90)90055-Q)
- Klais, R., T. Tamminen, A. Kremp, K. Spilling, and K. Olli. 2011. Decadal-scale changes of dinoflagellates and diatoms in the anomalous Baltic Sea spring bloom. *PLoS One* **6**: e21567. doi:[10.1371/journal.pone.0021567](https://doi.org/10.1371/journal.pone.0021567)
- Koskinen, K., J. Hultman, L. Paulin, P. Auvinen, and H. Kankaanpää. 2011. Spatially differing bacterial communities in water columns of the northern Baltic Sea. *FEMS Microbiol. Ecol.* **75**: 99–110. doi:[10.1111/j.1574-6941.2010.00987.x](https://doi.org/10.1111/j.1574-6941.2010.00987.x)
- Kuparinen, J., and H. Kuosa. 1993. Autotrophic and heterotrophic picoplankton in the Baltic Sea. *Adv. Mar. Biol.* **29**: 73–128. doi:[10.1016/S0065-2881\(08\)60130-3](https://doi.org/10.1016/S0065-2881(08)60130-3)
- Lane, D. J. 1991. 16S/23S sequencing, p. 171–204. *In* E. Stackebrandt and M. Goodfellow [eds.], *Nucleic acid techniques in bacterial systematics*. Wiley.
- Legrand, C., E. Fridolfsson, M. Bertos-Fortis, E. Lindehoff, P. Larsson, J. Pinhassi, and A. Andersson. 2015. Interannual variability of phyto-bacterioplankton biomass and production in coastal and offshore waters of the Baltic Sea. *Ambio* **44**: 427–438. doi:[10.1007/s13280-015-0662-8](https://doi.org/10.1007/s13280-015-0662-8)
- Lignell, R. 1990. Excretion of organic carbon by phytoplankton: Its relation to algal biomass, primary productivity and bacterial secondary productivity in the Baltic Sea. *Mar. Ecol. Progr. Ser.* **68**: 85–99. doi:[10.3354/meps068085](https://doi.org/10.3354/meps068085)
- Lindh, M. V., and others. 2015. Disentangling seasonal bacterioplankton population dynamics by high-frequency sampling. *Environ. Microbiol.* **17**: 2459–2476. doi:[10.1111/1462-2920.12720](https://doi.org/10.1111/1462-2920.12720)
- Lindh M. V., and J. Pinhassi. 2018. Sensitivity of Bacterioplankton to Environmental Disturbance: A Review of Baltic Sea Field Studies and Experiments. *Front. Marine Sci.* **5**. doi:[10.3389/fmars.2018.00361](https://doi.org/10.3389/fmars.2018.00361)
- Lipsewiers, T., and K. Spilling. 2018. Microzooplankton, the missing link in Finnish plankton monitoring programs. *Boreal Environ. Res.* **23**: 127–137.
- Liu, Y., P. Debeljak, M. Rembauville, S. Blain, and I. Obernosterer. 2019. Diatoms shape the biogeography of heterotrophic prokaryotes in early spring in the Southern Ocean. *Environ. Microbiol.* **21**: 1452–1465. doi:[10.1111/1462-2920.14579](https://doi.org/10.1111/1462-2920.14579)

- Logares, R. 2017 Workflow for analysing MiSeq amplicons based on Uparse v1.5. Zenodo 10, 5281. doi:[10.5281/zenodo.259579](https://doi.org/10.5281/zenodo.259579)
- Martin Marcel 2011. Cutadapt removes adapter sequences from high-throughput sequencing reads. EMBnet. J. **17**(1): 10. doi:[10.14806/ej.17.1.200](https://doi.org/10.14806/ej.17.1.200)
- Morán, X. A. G., and M. Estrada. 2002. Phytoplanktonic DOC and POC production in the Bransfield and Gerlache Straits as derived from kinetic experiments of ^{14}C incorporation. Deep Sea Res. II: Topical Stud. Oceanogr. **49**: 769–786. doi:[10.1016/s0967-0645\(01\)00123-0](https://doi.org/10.1016/s0967-0645(01)00123-0)
- Myklestad S. M. 1995. Release of extracellular products by phytoplankton with special emphasis on polysaccharides. Sci. Total Environ. **165**: 155–164. doi:[10.1016/0048-9697\(95\)04549-g](https://doi.org/10.1016/0048-9697(95)04549-g)
- Norland, S. 1993. The relationship between biomass and volume of bacteria, p. 303–307. In P. F. Kemp, B. F. Sherr, E. B. Sherr, and J. J. Cole [eds.], Handbook of methods in aquatic microbial ecology. Lewis.
- Olli, K., and K. Trunov. 2010. Abundance and distribution of vernal bloom dinoflagellate cysts in the Gulf of Finland and Gulf of Riga (the Baltic Sea). Deep Sea Res. II: Topical Stud. Oceanogr. **57**: 235–242. doi:[10.1016/j.dsr2.2009.09.009](https://doi.org/10.1016/j.dsr2.2009.09.009)
- Oswald, K., and others. 2017. Crenothrix are major methane consumers in stratified lakes. ISME J. **11**: 2124–2140. doi:[10.1038/ismej.2017.77](https://doi.org/10.1038/ismej.2017.77)
- Pérez, M. T., P. Hörtnagl, and R. Sommaruga. 2010. Contrasting ability to take up leucine and thymidine among freshwater bacterial groups: Implications for bacterial production measurements. Environ. Microbiol. **12**: 74–82. doi:[10.1111/j.1462-2920.2009.02043.x](https://doi.org/10.1111/j.1462-2920.2009.02043.x)
- Pinhassi, J., M. M. Sala, H. Havskum, F. Peters, O. Guadayol, A. Malits, and C. Marrasé. 2004. Changes in bacterioplankton composition under different phytoplankton regimens. Appl. Environ. Microbiol. **70**: 6753–6766. doi:[10.1128/AEM.70.11.6753-6766.2004](https://doi.org/10.1128/AEM.70.11.6753-6766.2004)
- R Development Core Team. 2008. R: A language and environment for statistical computing. R Foundation for Statistical Computing.
- Raes, J., I. Letunic, T. Yamada, L. J. Jensen, and P. Bork. 2011. Toward molecular trait-based ecology through integration of biogeochemical, geographical and metagenomic data. Mol. Syst. Biol. **7**: 473. doi:[10.1038/msb.2011.6](https://doi.org/10.1038/msb.2011.6)
- Richert, I., P. Yager, J. Dinasquet, R. Logares, L. Riemann, A. Wendeberg, S. Bertilsson, and D. G. Scofield. 2019. Summer comes to the Southern Ocean: How phytoplankton shape bacterioplankton communities far into the deep dark. Ecosphere **10**: e02641. doi:[10.1002/ecs2.2641](https://doi.org/10.1002/ecs2.2641)
- Rieck, A., D. P. Herlemann, K. Jürgens, and H. P. Grossart. 2015. Particle-associated differ from free-living bacteria in surface waters of the Baltic Sea. Front. Microbiol. **6**: 1297. doi:[10.3389/fmicb.2015.01297](https://doi.org/10.3389/fmicb.2015.01297)
- Sarmiento, H., and others. 2013. Phytoplankton species-specific release of dissolved free amino acids and their selective consumption by bacteria. Limnol. Oceanogr. **58**: 1123–1135. doi:[10.4319/lo.2013.58.3.1123](https://doi.org/10.4319/lo.2013.58.3.1123)
- Simon, M., and F. Azam. 1989. Protein content and protein synthesis rates of planktonic marine bacteria. Mar. Ecol. Prog. Ser. **51**: 201–213. doi:[10.3354/meps051201](https://doi.org/10.3354/meps051201)
- Smith, D. C., and F. Azam. 1992. A simple, economical method for measuring bacterial protein synthesis rates in seawater using ^3H -leucine. Mar. Microb. Food Webs **6**: 107–114.
- Spilling, K. 2007. On the ecology of cold-water phytoplankton in the Baltic Sea. PhD thesis. Univ. of Helsinki.
- Spilling, K., and S. Markager. 2008. Ecophysiological growth characteristics and modeling of the onset of the spring bloom in the Baltic Sea. J. Mar. Syst. **73**: 323–337. doi:[10.1016/j.jmarsys.2006.10.012](https://doi.org/10.1016/j.jmarsys.2006.10.012)
- Spilling, K., K. Olli, J. Lehtoranta, A. Kremp, L. Tedesco, T. Tamelander, R. Klais, H. Peltonen, and T. Tamminen. 2018. Shifting diatom—dinoflagellate dominance during spring bloom in the baltic sea and its potential effects on biogeochemical cycling. Front. Marine Sci. **5**. doi:[10.3389/fmars.2018.00327](https://doi.org/10.3389/fmars.2018.00327)
- Spilling K., A. Fuentes-L., D. Quemaliños, R. Klais, and C. Sobrino. 2019. Primary production, carbon release, and respiration during spring bloom in the Baltic Sea. Limnol. Oceanogr. doi:[10.1002/lno.11150](https://doi.org/10.1002/lno.11150)
- Steemann-Nielsen, E. 1952. The use of radio-active carbon (^{14}C) for measuring organic production in the sea. ICES J. Mar. Sci. **18**: 117–140. doi:[10.1093/icesjms/18.2.117](https://doi.org/10.1093/icesjms/18.2.117)
- Stoecker, K., and others. 2006. Cohn's Crenothrix is a filamentous methane oxidizer with an unusual methane monooxygenase. Proc. Natl. Acad. Sci. USA **103**: 2363–2367. doi:[10.1073/pnas.0506361103](https://doi.org/10.1073/pnas.0506361103)
- Sundström, A. M., A. Kremp, N. Daugbjerg, Ø. Moestrup, M. Ellegaard, R. Hansen, and S. Hajdu. 2009. *Gymnodinium corollarium* sp. nov.(dinophyceae)—a new cold-water dinoflagellate responsible for cyst sedimentation events in the Baltic Sea. J. Phycol. **45**: 938–952. doi:[10.1111/j.1529-8817.2009.00712.x](https://doi.org/10.1111/j.1529-8817.2009.00712.x)
- Tamminen, T., and T. Andersen. 2007. Seasonal phytoplankton nutrient limitation patterns as revealed by bioassays over Baltic Sea gradients of salinity and eutrophication. Mar. Ecol. Prog. Ser. **340**: 121–138. doi:[10.3354/meps340121](https://doi.org/10.3354/meps340121)
- Teeling, H., and others. 2012. Substrate-controlled succession of marine bacterioplankton populations induced by a phytoplankton bloom. Science **336**: 608–611. doi:[10.1126/science.1218344](https://doi.org/10.1126/science.1218344)
- Wichard, T., S. A. Poulet, and G. Pohnert. 2005. Determination and quantification of α , β , γ , δ -unsaturated aldehydes as pentafluorobenzyl-oxime derivatives in diatom cultures and natural phytoplankton populations: Application in

- marine field studies. *J. Chromatogr. B* **814**: 155–161. doi:[10.1016/j.jchromb.2004.10.021](https://doi.org/10.1016/j.jchromb.2004.10.021)
- Wolter, K. 1982. Bacterial incorporation of organic substances released by natural phytoplankton populations. *Mar. Ecol. Prog. Ser.* **7**: 287–295. doi:[10.3354/meps007287](https://doi.org/10.3354/meps007287)
- Zhang, J., K. Kobert, T. Flouri, and A. Stamatakis. 2014. PEAR: A fast and accurate Illumina Paired-End reAd mergeR. *Bioinformatics* **30**: 614–620. doi:[10.1093/bioinformatics/btt593](https://doi.org/10.1093/bioinformatics/btt593)

Acknowledgments

This study was funded by the Walter and Andrée de Nottbeck Foundation and the Academy of Finland (decision numbers 259164 and 292711). The study utilized SYKE marine research infrastructure as a part of the national FINMARI consortium. We would like to thank the staff at

Tvärminne Zoological Station and the staff on board the Aranda vessel for help with the analytical measurements and sampling during the experiments. Clara Ruiz González was supported by the GRAMMI project (RTI2018-099740-J-I00, MICIU, Spain).

Conflict of Interest

None declared.

Submitted 18 September 2019

Revised 29 April 2020

Accepted 20 August 2020

Associate editor: Tatiana Rynearson